Characterization technique for inhomogeneous 4H-SiC Schottky contacts: A practical model for high temperature behavior

G. Brezeanu,[1] G. Pristavu,[1] F. Draghici,[1] M. Badila,[1] and R. Pascu[2]
[1]*Electronics, Telecommunications and Information Technology, University Politehnica Bucharest, Bucharest 061071, Romania*
[2]*National Institute for Research and Development in Microtechnologies, Erou Iancu Nicolae Street 126A, 077190 Bucharest, Romania*

(Received 23 March 2017; accepted 5 August 2017; published online 22 August 2017)

In this paper, a characterization technique for 4H-SiC Schottky diodes with varying levels of metal-semiconductor contact inhomogeneity is proposed. A macro-model, suitable for high-temperature evaluation of SiC Schottky contacts, with discrete barrier height non-uniformity, is introduced in order to determine the temperature interval and bias domain where electrical behavior of the devices can be described by the thermionic emission theory (has a quasi-ideal performance). A minimal set of parameters, the effective barrier height and p_{eff}, the non-uniformity factor, is associated. Model-extracted parameters are discussed in comparison with literature-reported results based on existing inhomogeneity approaches, in terms of complexity and physical relevance. Special consideration was given to models based on a Gaussian distribution of barrier heights on the contact surface. The proposed methodology is validated by electrical characterization of nickel silicide Schottky contacts on silicon carbide (4H–SiC), where a discrete barrier distribution can be considered. The same method is applied to inhomogeneous Pt/4H–SiC contacts. The forward characteristics measured at different temperatures are accurately reproduced using this inhomogeneous barrier model. A quasi-ideal behavior is identified for intervals spanning 200 °C for all measured Schottky samples, with Ni and Pt contact metals. A predictable exponential current-voltage variation over at least 2 orders of magnitude is also proven, with a stable barrier height and effective area for temperatures up to 400 °C. This application-oriented characterization technique is confirmed by using model parameters to fit a SiC-Schottky high temperature sensor's response. *Published by AIP Publishing*. [http://dx.doi.org/10.1063/1.4999296]

I. INTRODUCTION

Schottky barrier diodes (SBDs) are cost-effective devices, which operate with very fast switching speeds and low turn-on voltages when compared to *pn* diodes, due to their reliance solely on majority carrier transport, free of the recombination mechanism. This makes the Schottky diode a general choice in applications such as switched mode power supplies, RF, voltage clamping, and extensively in sensor electronics.[1–7]

Silicon carbide (SiC) exhibits an intrinsic carrier concentration several orders of magnitude lower than Si, with the consequent reduction of leakage current and increase in maximum device operating temperature. The possibility to operate at elevated temperatures, combined with a high thermal conductivity and high radiation and chemical tolerance, offers many possibilities for using SiC as a material for a wide range of devices and sensors—particularly in applications featuring high temperatures or hostile environments.[1,4] A factor which limits the proliferation of SiC devices is ultimately cost, SiC Schottky diodes being up to five times more expensive than their fast-recovery Si-based counterparts.[1,5,6] This issue restricts the use of wide-bandgap Schottky devices to high temperature applications, where other solutions simply cannot operate.

The criteria for obtaining accurate SiC-Schottky diodes, capable of operating over extended temperature ranges, are well established: elevated and temperature independent Schottky barrier height (SBH), low series resistance, and large contact area.[1–5] However, virtually all research regarding the behavior of SBDs in high-temperature sensing and power applications over large intervals has emphasized the spurious effect of contact inhomogeneity and barrier non-uniformity.[1,3,8–52] It is very important to consider and model how current passes through a non-uniform contact, as well as how this impacts device electrical characteristics across wide temperature and voltage ranges, for various interfaces of differing quality and uniformity. As technology matures and manufacturing is performed on wafers of increasing sizes,[1] an essential focus for bridging the gap between costs for SiC and Si components becomes the improvement of yield. Non-uniformity modeling and accurate, phenomenological device characterization are expected to become instrumental in order to reach this goal.

This paper analyzes shortcomings of the conventional Schottky diode characterization technique, regarding non-uniform contacts, discusses existent inhomogeneity models and focuses on an alternative assessment method, suitable for determining the temperature range and bias domain where the electrical behavior can be described by the thermionic emission (TE) theory. For these intervals, despite contact inhomogeneity, the devices may be considered standard Schottky diodes, with exponential forward characteristics, adequate for a large array of practical applications. This method is based on a macroscopic multi-barrier Schottky

contact model which brings in a single parameter (p_{eff}) to describe the contact surface non-uniformity. The standard SBH evaluation approach is employed in tandem with model-adjusted Arrhenius plots, in order to obtain the ideality factor, the effective barrier, and non-uniformity parameter, respectively.

High-barrier SiC-Schottky diodes, with Ni and Pt contact metals, are fabricated, measured up to 400 °C and characterized using the proposed technique. Even devices with high degrees of contact non-uniformity are proven to behave predictably in operating ranges spanning over 200 °C. For these intervals, bias regions where the diodes exhibit quasi-ideal current-voltage dependence, with a stable barrier and effective area, are identified.

Section II discusses non-uniform Schottky contacts regarding formation causes, conventional characterization techniques, and existing inhomogeneity models, comparing literature results for a variety of metal-SiC interfaces. A simple macro-model of a non-uniform Schottky contact, valid for high-temperature operation, is proposed in Sec. III. In Sec. IV, a complete technique for inhomogeneous contact characterization is developed. A very good agreement of the measured forward I-V characteristics, for SiC-Schottky diodes with Ni and Pt contact metals, selected for their varying degrees of inhomogeneity, with fitted curves, based on parameters of the proposed model, is performed. The physical relevance of extracted parameters is discussed and confirmed for high-temperature applications. Final considerations are presented and conclusions are drawn in Sec. V.

II. SCHOTTKY CONTACT NONUNIFORMITY

In the last few decades, the scientific community has seen an impressive increase in the literature regarding Schottky contacts on wide band-gap semiconductors, such as silicon carbide, gallium nitride, or diamond.[1,14] In the case of SiC, the driving force behind progress was that the semiconductor is highly suitable for hostile environment operation, while offering a band gap large enough to produce devices with very high temperature capabilities.[1,3,9–12] Even though Schottky diodes are usable in a large array of applications, the switching and sensing properties are what made them consecrated and widely investigated devices, with extensive research effort being invested in modeling and characterizing the metal-semiconductor contact.[1–4,8–13,16–52]

The I_F-V_F-T characteristic for an ideal Schottky diode is given by the thermionic emission (TE) equation[1–4,8–13,16–52]

$$I_F \cong I_S \exp\left(\frac{V_F - I_F R_S}{n V_{th}}\right), \tag{1}$$

where R_S is the series resistance, n is the ideality factor, V_{th} is the thermal voltage, and I_S is the saturation current

$$I_S \cong A_n A_S T^2 \exp\left(-\frac{\Phi_{Bn,T}}{V_{th}}\right). \tag{2}$$

In Eq. (2), A_S is the nominal contact area, A_n is the Richardson constant for electrons (146 $A/K^2 cm^2$ for 4H-SiC[31]), and $\Phi_{Bn,T}$ is the conventional Schottky barrier height. The Schottky diode parameters are often obtained based on I_F-V_F characteristics measured at constant temperature using the nominal area as a design parameter. This analysis is the overwhelmingly preferred method, present in virtually all literature pertaining to SiC-Schottky diode characterization.[1–4,8–13,16–52] The conventional barrier and the ideality factor are determined from the y-axis intercept and slope of the linear fit of $\ln(I_F)$ as a function of V_F curve, respectively, using Eqs. (1) and (2).

We may define a "homogeneous" metal-semiconductor Schottky contact as one with a single barrier ($\Phi_{Bn,T}$) and ideality factor n close to 1. According to the TE mechanism, $\Phi_{Bn,T}$ and n should be reasonably temperature and voltage independent.

When the forward characteristics of real Schottky contacts were modeled with this ideal metal semiconductor contact theory [Eq. (1)] over extended temperature ranges, the presence of anomalous behavior was always evinced. Most common was the presence of large ideality factors, often at low temperature, and a significant variation of the Schottky barrier and ideality factor with temperature and bias voltage. These spurious effects were attributed to inhomogeneity present on the contact, due to doping non-uniformity, elevated interface state density,[44] surface defects, mixture of different metal semiconductor phases,[37] etc. Also, because the interface between the metal and semiconductor is not atomically flat, the built-in potential and the barrier height are expected to fluctuate spatially.[36–38,48]

In the case of metal/SiC interactions, a wide variety of reactions, resulting after the usual post-metallization annealing process, have been reported,[15,50] leading to contact inhomogeneity. The classification includes non-reactive metals, such as Ag or Au, materials that form only silicides (Co, Ni, Pd, Pt, etc.) and metals that react into both silicide and carbide (Cr, Fe, Mn, W, etc.), as well as materials that are able to yield a ternary phase (Mo, Ta, Ti, Zr, etc).[15,50] At the same doping concentration, all these phases can have different Schottky barrier heights and specific contact resistances. For Schottky contacts on n-type SiC, Ni, Pt, and Pd silicides are the most used metals since their high work function should result in a high value of the Schottky barrier.

The SBH variations have a major impact on the performances of SiC Schottky diodes in switching and sensing applications, leading to abnormally high leakage currents (considerably increasing switching losses), as well as deteriorating linearity and sensitivity in gas and temperature monitoring.

In order to account for barrier inhomogeneity, the most prominent model used assumes that a non-uniform contact behaves essentially as multiple diodes connected in parallel, each with its own specific barrier height, effective area, and series resistance. This approach was proposed by Song *et al.*[36] and followed by Werner and Güttler,[37] who first introduced the analytical function potential fluctuations in the thermionic emission model. According to this method, for a real metal-semiconductor contact, the SBH spatial variations follow a Gaussian distribution, leading to a temperature dependence of the conventional barrier[37]

$$\Phi_{Bn,T} = \Phi_{Bn}^{0} - \frac{\sigma^2}{2V_{th}}, \quad (3)$$

where Φ_{Bn}^{0} is the mean barrier value and σ is the dispersion of the Gaussian distribution.

The parallel conduction model was completed by Tung through the incorporation of the "pinch-off" effect, which takes into account the interaction between different regions when their barrier heights vary spatially on a scale comparable to the space-charge region width.[38]

According to these models, an inhomogeneous Schottky contact can be described like a distribution of low-barrier patches embedded in an ideal uniform high-barrier region. Under these conditions, the current flow through the high-barrier regions becomes dominant only at high temperature. Since, in this case, the carriers overcome the highest barrier by a nearly pure TE mechanism,[22,31] it is expected that the behavior of a non-uniform contact will approach ideality as temperature increases.

The inhomogeneity theory based on a SBH Gaussian distribution has been validated for a large number of Schottky contacts. Table I summarizes some model SBH values for various real Schottky contacts reported in the literature.

In every case, the annealing treatment of the Schottky contact and temperature range, where diode current-voltage characteristics were measured, are emphasized. Differences between $\Phi_{Bn,T}$ [obtained with Eq. (1)] and mean barrier heights [resulting from Eq. (3)] can be observed, resulting from different contact types, annealing temperatures, investigated domains, and analysis methods. As an example, for annealed Ni/SiC Schottky contacts, the coexistence of difference nickel silicide phases ($Ni_{31}Si_{12}$, Ni_2Si,…) at the interface and/or the redistribution of carbon precipitates inside the reacted layer can explain the degree of inhomogeneity of the contact and the various SBH values reported (Table I).

The smallest values were achieved for the effective barrier ($\Phi_{Bn,eff}$), extracted from the standard Richardson curve. This representation is $\ln\left(\frac{I_S}{T^2}\right)$ as a function of $\frac{1}{T}$, where T is the absolute temperature, also known as an Arrhenius (activation energy) plot. From the slope of the straight line, the effective barrier is obtained, while from the y-axis intercept, the value of Richardson's constant (A_n) is determined. It should be noted that enormous differences, between extracted values for this constant and the theoretical one, were reported. This was a direct result of using the nominal area as input data.[16,31,45] When applying the Gaussian distribution models,[37,38] a gap-closing between the theoretical and extracted values of Richardson's constant was attempted by introducing the *modified* Richardson plot, $\ln\left(\frac{I_S}{T^2}\right) - \frac{\sigma^2}{2V_{Th}^2}$ versus $\frac{1}{T}$, where σ is an essential parameter of the Gaussian distribution approach. The barrier extracted from the slope of this linear dependence became very close to the mean barrier ($\Phi_{Bn}^{0} \cong \Phi_{Bn,eff}$), now. This coincidence served to further establish the validity of the inhomogeneity model.

Existing inhomogeneity models have proven themselves accurate for fitting experimental data. Tung's "pinch-off" model, coupled with resistive effects, was employed by Gammon *et al.*[16] to fully recreate recorded I-V curves over a very wide low-temperature range (20 K–320 K), (Table I, Row 2). Furthermore, Gülnahar recently demonstrated compatibility between Tung's method and a multi-Gaussian distribution approach when analyzing highly inhomogeneous SiC Schottky devices at cryogenic temperatures[45] (Table I). Despite these encouraging results, accurate reproduction of measured data was only possible by segregating model parameters to temperature intervals where they are most relevant, essentially attributing different current flow equations to these domains.[16] Also, as Gammon himself points out, "close scrutiny of the fitting data used in both methods leaves questions about what physical interpretation should be drawn from the fitting parameters of either model."[16] Using various, large numbers of fitting parameters, without physical significance, greatly encumbers the characterization process for SiC Schottky diodes targeted at applications over wide temperature ranges. More so, the punctilious approach rather indicates the incontrollable and unpredictable behavior of the devices, greatly discrediting their ability to far exceed the temperature capabilities of conventional semiconductor diodes. Unsurprisingly, commercially available SiC-Schottky diodes are largely restricted to operating temperatures up to 175 °C, even if adequate packaging technologies were demonstrated up to at least 250 °C.[53,54]

When looking to fully exploit the advantages of SiC devices over silicon-based solutions, application-oriented characterizing techniques must be developed, with a minimal set of physically relevant parameters, allowing seamless

TABLE I. Literature SBH data obtained with different models for some real 4H-SiC Schottky contacts.

Schottky contact	Annealing	Investigated temperature range	Conventional barrier ($\Phi_{Bn,T}$)	Mean barrier (Φ_{Bn}^{0})	Effective barrier ($\Phi_{Bn,eff}$) (V)	Source
Ni/4H-SiC	No annealing	40 K–300 K	0.37 V–1.44 V	~1.65 V	0.91	43
Ni/4H-SiC	No annealing	20 K–320 K	0.1 V–0.935 V	0.76 V–1 V	…	16
Ni/4H-SiC	550 °C	27 °C–400 °C	~1.5 V	…	…	51
Ni/4H-SiC	700 °C	98 K–473 K	1.31 V–1.66 V	1.69 V	1.5	31
Pt/4H-SiC	200 °C–1000 °C	Room	1 V–1.7 V	…	…	46
Au/4H-SiC	No annealing	50 K–300 K	0.93 V–1.18 V	1.24 V/1.36 V	0.98	45
Mo/4H-SiC	500 °C	25 °C–225 °C	1.01 V–1.07 V	1.14 V–1.16 V	0.9	44
W/4H-SiC	500 °C	30 °C–175 °C	1.11 V–1.17 V	1.28 V	1	48
Ti/4H–SiC	No annealing	173 K–373 K	1.24 V–1.27 V	1.31 V	1.22	31

integration in the manufacturing flow. While complexity should be kept to a minimum, models used by these techniques need to be capable of eliminating the short comings of the homogeneous barrier-assuming conventional methods.

In many practical situations, the Schottky contact results following post metallization annealing treatments at various temperatures. The annealing is explicitly carried out in order to favor the formation of a specific (mainly silicide) phase. These sintering processes lead to the consumption of the original defect-prone interface and the creation of a new, significantly more uniform Schottky contact. However, even if room-temperature measurements on annealed devices indicated adequate behavior, extending investigations to a wider temperature range suggested that an inhomogeneous contact had still been formed.[1,3,31,42,46] It can be expected that a real SiC-Schottky contact have a mix of different compounds present on its surface. This effect is much more impactful for SiC than for Si based devices due to increased reaction diversity and extended operation temperature range. It should be noted that, for the Pt/SiC contact (Table I), no inhomogeneity model was applied.[46] In this case, only the conventional barrier was extracted, at room temperature. The Pt data (Table I) are relevant because they emphasize a strong impact of the annealing process on diode electrical behavior.

Analyzing results in Table I showed that barrier variations are way more pronounced for contacts with no annealing. In those cases, existing Gaussian-distribution-based models are adequate due to the incontrollable shape of the interface. For annealed Schottky contacts, the interface quality is greatly improved and many causes for SBH continuous temperature variation are removed.[31,42] The main reason for barrier non-uniformity becomes the presence of distinct regions associated with different phases on the contact's surface. It should be noted that, for high temperature operation, Shottky contact annealing is mandatory, in order to prevent partial sintering on its surface and maintain stable electrical behavior.[1] Thus, when looking to properly characterize SiC Schottky diodes at elevated temperatures, a discrete contact composition approach can be considered, with sizeable simplifications from existing inhomogeneity models.

Figure 1 illustrates the electrical behavior of a simulated non-uniform Schottky contact with three metal-SiC phase regions, having different SBH and widely different areas (specified in the legend in Fig. 1). The simulated saturation current variations with temperature [calculated by Eq. (2)] for each region of this 3-barrier diode are given in Fig. 1(a). The associated contributions of these zones to total Schottky contact current are shown in Fig. 1(b) and temperature dependence of the conventional Schottky barrier for the overall diode is presented in Fig. 1(c).

The majority current (over 80%) for this 3-barrier diode will be flowing through the lower barrier patch until 27 °C, even if its active area is several orders of magnitude lower than the entire diode surface [dashed plot—Fig. 1(b)]. Above 150 °C, the current through the medium barrier ($\Phi_{Bn,m} = 1.15$ V) region becomes dominant [dotted plot—Fig. 1(b)]. The zone occupying the vast majority of the contact surface will overtake conduction above 500 °C, only [continuous curve—Fig. 1(b)]. The effective area conducting

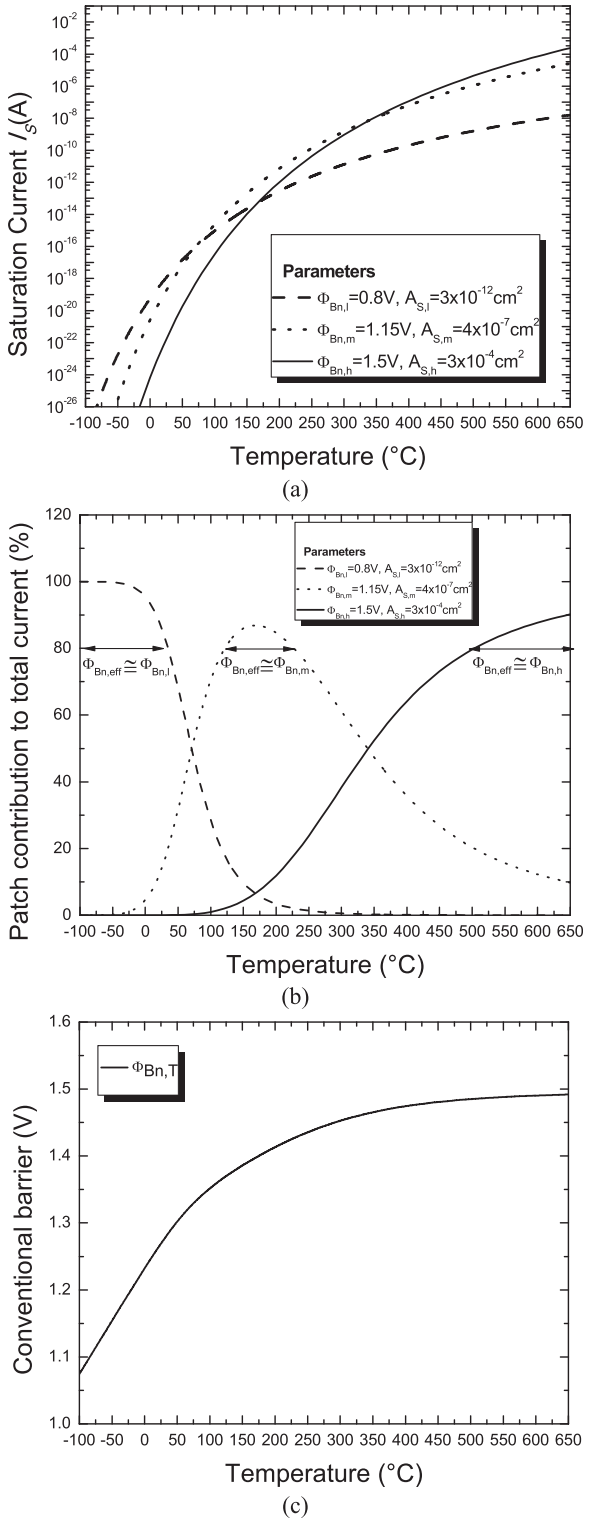

FIG. 1. (a) Saturation current of each of the three regions versus temperature for the simulated 3-barrier diode. (b) Associated contribution of all regions to total current. (c) Conventional barrier temperature variation of the overall Schottky diode.

most of the device's current not only differs from the designed value, but it also changes with the temperature range. In fact, at very high temperatures, current flows predominantly through the largest area zone, regardless of the barrier height value. For this reason, extracting the effective Schottky barrier of an inhomogeneous contact at different

temperatures becomes impossible using the conventional method, as proven by the plot in Fig. 1(c). The conventional barrier $\Phi_{Bn,T}$ reaches physically relevant values barely when the highest area region contributes predominantly to current through the contact, i.e., at high temperatures, only.

In Sec. III, a macro-model, accurate for high-temperature characterization of SiC Schottky diodes, with similar non-uniformity discrete distributions to the above-simulated device, is proposed. A minimal set of parameters, allowing the quick assessment of the degree of contact inhomogeneity, is associated. Very importantly, the temperature range and bias interval, where quasi-ideal diode behavior can be considered, are established.

III. MODEL

The starting point of our model is Werner and Guttler's version, where it is assumed that the Schottky contact comprises a set of multiple ideal (fully homogeneous) regions with different barrier heights ($\Phi_{Bn,i}$) and effective areas, represented as a fraction of the total contact area: $A_i = A_S/a_i$. It should be noted that the ideality factors for each region are considered very close to unity, as it was proven by Tung[38] that n cannot deviate past 1.03 as a result of effects other than contact inhomogeneity.

The model is associated with the above room-temperature ranges, where the field emission or TE assisted by field emission diode current components are negligible. At these elevated temperatures, patches under the influence of the "pinch-off" effect[38] should contribute very little to the overall current flow due to their minuscule surface and increased apparent SBH.[8,31,38,45] Thus, the total current through an inhomogeneous contact is obtained through summation of all region contributions, according to the thermionic emission law:

$$I_F \cong \sum_{i=1}^{m} A_i A_n T^2 \exp\left(-\frac{\Phi_{Bn,i}}{V_{th}}\right)\exp\left(\frac{V_F}{nV_{th}}\right) = A_n A_S T^2 \exp\left(\frac{V_F}{nV_{th}}\right)\exp\left(-\frac{\Phi_{Bn,l}}{V_{th}}\right)\sum_{i=1}^{m}\frac{1}{a_i}\exp\left(-\frac{\Delta\Phi_{Bn,i}}{V_{th}}\right), \tag{4}$$

where m is the number of different-barrier regions, $\Phi_{Bn,l}$ is the lowest barrier present on the contact surface and $\Delta\Phi_{Bn,i} = \Phi_{Bn,i} - \Phi_{Bn,l}$. In practice, it is assumed that the highest area region (a_{MAX}) has a desired/designed barrier height ($\Phi_{Bn,d}$). For a uniform contact, $a_{MAX} \cong 1$.

The expression for the conventional barrier height ($\Phi_{Bn,T}$) can be determined using Eqs. (1), (2), and (4)

$$\Phi_{Bn,T} \cong \Phi_{Bn,l} - V_{th}\ln\sum_{i=1}^{m}\frac{1}{a_i}\exp\left(-\frac{\Delta\Phi_{Bn,i}}{V_{th}}\right). \tag{5}$$

The limits of variation for $\Phi_{Bn,T}$ are imposed by the temperature range. The complete steps for calculating these limits are presented in the Appendix. A zero temperature barrier limit is

$$\Phi_{Bn,T}|_{V_{th}\to 0} = \lim_{V_{th}\to 0}\left[\Phi_{Bn,l} - V_{th}\ln\sum_{i=1}^{m}\frac{1}{a_i}\exp\left(-\frac{\Delta\Phi_{Bn,i}}{V_{th}}\right)\right] = \Phi_{Bn,l}. \tag{6}$$

The upper limit for $\Phi_{Bn,T}$ is reached at very high temperatures ($V_{th}\to\infty$)

$$\Phi_{Bn,T}|_{V_{th}\to\infty} = \sum_{i=1}^{m}\frac{\Phi_{Bn,i}}{a_i} \cong \Phi_{Bn,d}. \tag{7}$$

This sum represents an average of barriers afferent to all m zones present on the contact surface, each weighted by the area of the region. It is the saturation point of $\Phi_{Bn,T}$, reached at very high temperatures. For a quasi-uniform Schottky contact (where $a_{MAX} \cong 1$), there are relatively small differences between $\Phi_{Bn,i}$ and the term $\left(\frac{\Phi_{Bn,d}}{a_{MAX}}\right)$ will accurately approximate the entire sum in (7). For fully uniform barrier contacts, the conventional barrier is practically constant with temperature

$$\Phi_{Bn,T} = \Phi_{Bn,d} = \text{const.} \tag{8}$$

It is noted that the conventional barrier value obtained by Eq. (7) (at very high temperatures) is the discrete equivalent of the mean barrier in the Gaussian distribution approach,[37] because, in Eq. (3), $\Phi_{Bn,T}|_{V_{th}\to\infty} = \Phi_{Bn}^0$. Often however, because of the series resistance, the maximum operating temperature of a Schottky diode may be insufficient to ensure that the desired barrier region becomes dominant for current conduction. In this case, neither the conventional nor the mean barrier can properly reflect the real behavior of the device, often fallaciously indicating the inadequacy of the diode for high temperature applications.

We've previously[1,10] introduced a simple and intuitive model for inhomogeneous contacts which assumes current conduction through two regions with two different barriers, only. According to this model, the I_F-V_F-T characteristic of an inhomogeneous diode is also given by the TE expression

$$I_F \cong A_n A_S T^2 \exp\left(\frac{V_F}{nV_{th}}\right)\exp\left(-p - \frac{\Phi_{Bn,l}}{V_{th}}\right), \tag{9}$$

where $\Phi_{Bn,l}$ is the lowest barrier, and p defined as[10]

$$p = -\ln\left[\frac{1}{a_l} + \frac{1}{a_h}\exp\left(-\frac{\Delta\Phi_{Bn}}{V_{th}}\right)\right], \tag{10}$$

represents a parameter which quantitatively assesses the degree of non-uniformity.[10] In Eq. (10), a_l and a_h are the ratios between designed area (A_S) and low and high barrier region surfaces, respectively.[10] $\Delta\Phi_{Bn}$ is the difference between the barriers of the two zones.

The improved model, proposed in this paper, is based on Eqs. (4) and (5) and represents a generalization of the simple two barrier model [Eq. (9)]. Thus, to the non-uniformity parameter p is attributed an improved relationship, incorporating the effects of multiple barriers on the Schottky contact. Equations (4) and (5) yield

$$p = -\ln\left[\sum_{i=1}^{m}\frac{1}{a_i}\exp\left(-\frac{\Delta\Phi_{Bn,i}}{V_{th}}\right)\right]. \quad (11)$$

The definition form for parameter p enables the exploitation of a particular property for such equations. The *log-sum-exp* type expression [Eq. (11)] can be very accurately estimated by a single term for certain temperature intervals

$$p \cong \frac{\Delta\Phi_{Bn,i}}{V_{th}} - \ln\left(\frac{1}{a_i}\right). \quad (12)$$

In these distinct temperature ranges, the conventional barrier is approximated by

$$\Phi_{Bn,T} \cong \Phi_{Bn,l} + \Delta\Phi_{Bn,i} - \ln\left(\frac{1}{a_i}\right)V_{th} = \Phi_{Bn,i} - \ln\left(\frac{1}{a_i}\right)V_{th} = \Phi_{Bn,eff} + p_{eff}V_{th}, \quad (13)$$

which leads to a current expression through the inhomogeneous device of

$$I_F \cong A_n A_{eff} T^2 \exp\left(-\frac{\Phi_{Bn,eff}}{V_{th}}\right)\exp\left(\frac{V_F}{nV_{th}}\right). \quad (14)$$

Here,

$$A_{eff} = A_i = A_s\exp(-p_{eff}) = \frac{A_s}{a_i}. \quad (15)$$

This is the behavior of a single, ideal diode, with a SBH of $\Phi_{Bn,eff}$ and effective area of A_S/a_i.

The proposed model permits the determination of both p_{eff} and $\Phi_{Bn,eff}$ using an Arrhenius plot (or activation energy plot,[1,10–13,31]) of forward characteristics measured at different temperatures and a constant V_F[1,10]

$$\ln\left(\frac{I_F}{A_n A_S T^2}\right) = -p_{eff} - \left(\frac{\Phi_{Bn,eff}}{V_{th,0}} - \frac{V_F}{nV_{th,0}}\right)\frac{T_0}{T}. \quad (16)$$

Equation (16) is only valid for the temperature interval in which the simplified expression for p [Eq. (12)] is accurate. Furthermore, in this specific case, the effective barrier and p_{eff} are temperature independent, making Eq. (16) a linear dependence. Hence, both parameters may be extracted from the slope and intercept of the resulting line, respectively.

In the temperature range where Eq. (12) holds true, measured I_F-V_F characteristics are precisely fitted by calculated curves using Eqs. (14) and (15). The result is essential because it establishes the domains where a non-uniform diode has a near-ideal, predictable behavior and is therefore suitable in applications.

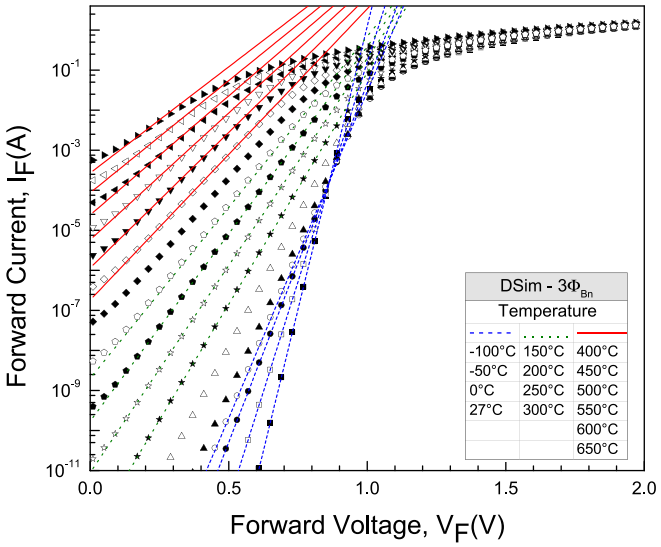

FIG. 2. Simulated I-V curves for $3\Phi_{Bn}$ diode versus fitted results using the activation energy p-method.

A preliminary validation of the above model is shown in Fig. 2, which depicts a comparison between forward characteristics for the simulated 3-barrier diode from Fig. 1 and fitted I-V curves [calculated using Eqs. (1), (2) and (13)]. The results of the comparative analysis are given in Table II. An excellent agreement between the simulated and model-calculated plots can be observed. This accurate matching was possible only by dividing the complete interval into three subdivisions, associated with the maximum current contribution temperature domains of each barrier region from Fig. 1(b). The goodness of fit, given by R^2, was over 99.9% in all cases. A different set of p_{eff} and $\Phi_{Bn,eff}$ values was extracted for each interval.

At low temperatures (−100 °C–27 °C), where the region with $\Phi_{Bn,l} = 0.8$ V contributes over 99% of total current through the contact, the extracted model parameters exactly match their physical counterparts ($\Phi_{Bn,eff} = \Phi_{Bn,l}$ and $A_{eff} = A_l$). Here, the very high value obtained for p_{eff} confirms the gross differences between A_{eff} and total contact area ($A_S \cong 3 \times 10^{-4}$ cm^2), considered in the model. If region area A_l (with SBH $\Phi_{Bn,l}$) would instead be used as the nominal area, a $p_{eff} \cong 0$ value will be obtained.

For higher temperatures, because dominant regions give only 80%–90% of total current [Fig. 1(b)], slight barrier

TABLE II. 3 barrier diode. Parameters for simulated versus model-fitted I-V curves.

Temperature range/parameter	−100 °C–27 °C	150 °C–300 °C	400 °C–650 °C
$\Phi_{Bn,eff}$	0.8 V	1.17 V	1.43V
Barrier (Fig. 1)	$\Phi_{Bn,l} = 0.8$ V	$\Phi_{Bn,m} = 1.15$ V	$\Phi_{Bn,h} = 1.5$ V
p_{eff}	18.42	5.77	0.78
A_{eff} (cm^2)	3×10^{-12}	9.3×10^{-7}	1.3×10^{-4}
Patch area (Fig. 1)	$A_l = 3 \times 10^{-12}$ cm^2	$A_m = 4 \times 10^{-7}$ cm^2	$A_h = 3 \times 10^{-4}$ cm^2

discrepancies occur (under 5%). This is also the reason why the extracted A_{eff} values differ from dominant region areas (Table II).

An important observation is that the characterization method based on the proposed model is able to identify stable barrier and area values even in temperature intervals where current conduction is not predominantly determined by a single-barrier region. Thus, for the 400 °C–500 °C range, where zones with $\Phi_{Bn,m} = 1.15$ V and $\Phi_{Bn,h} = 1.5$ V have comparable influence on total current [Fig. 1(b)], excellent fitting was achieved for $\Phi_{Bn,eff} = 1.43$ V and $p_{eff} = 0.78$. The non-uniformity parameter value leads to an effective area ($A_{eff} = 1.3 \times 10^{-4}$ cm^2) close to that of the higher-barrier surface.

This explains why the temperature domains given in Table II (and Fig. 2) are wider than those from Fig. 1(b). Thus, our model offers an effective tool for inhomogeneous contact characterization, providing accurate, physically relevant barrier values, together with an indication of the non-uniformity degree via the p_{eff} parameter.

IV. PROPOSED CHARACTERIZATION TECHNIQUE. MODEL VALIDATION

In order to experimentally demonstrate the effectiveness of the proposed characterization technique, two batches of 4H-SiC Schottky diodes with Ni_2Si and Pt/SiC contacts were fabricated. The selected Schottky metals were preferred due to their ability to form high quality metal-semiconductor interfaces and the elevated values for the Schottky barriers, which allow devices to operate at high temperatures (over 400 °C).

The Ni/SiC Schottky diodes were fabricated on an *n*-4H-SiC wafer with an approximately 2×10^{16} cm^{-3} doped and 8 μm thick epitaxial layer. For the Pt/4H-SiC Schottky diodes, the same *n*-type wafer with an 8 μm epitaxial layer having a doping concentration of 1.3×10^{16} cm^{-3} was used. After a RCA cleaning process, a thick layer (1 μm) of SiO_2 was deposited by LPCVD (Low-Pressure Chemical Vapor Deposition), in order to passivate the entire surface of the wafer. The active areas, with circular windows of 200 μm and 400 μm diameters, were opened in this deposited oxide using a solution based on ammonium fluoride and acetic acid. Hence, an oxide ramp profile (with a very small angle, <5°) which ensures a good uniformity of current density and a higher breakdown voltage of the SiC device was delimited.[1] The Schottky contacts were obtained after a Ni (150 nm) deposition process by sputtering. A thermal annealing, at 800 °C for 8 min, in a N_2 ambient atmosphere, was performed. A high barrier Ni_2Si region on the Schottky nominal area was identified by XRD spectroscopy.[10,55] On such designed surfaces, patches of different nickel silicide phases, forming contacts with a lower barrier, were previously reported,[31,42]

To obtain a Pt Schottky contact, a thin Pt film of 50 nm was deposited also by sputtering. The Schottky metal was defined by using the lift-off technique, followed by an annealing at 600 °C in an Ar atmosphere for 5 min. Finally, for both types of Schottky structures, a metallic stack of Cr (20 nm)/Au (100 nm) was deposited on both sides of the wafer, providing the pad, on the front, and ohmic contacts (on the backside).

The test samples were packaged in TO 39 capsules using wire bonding technology. The I_F-V_F characteristics of encapsulated diodes were measured at several temperatures up to 400 °C using a Keithley 4200 semiconductor characterization system.[1]

Figure 3 illustrates forward characteristics, at different temperatures, for four Ni/4H-SiC samples, selected to exhibit a comprehensive array of inhomogeneity-specific behavior. The contact diameters are indicated for every diode.

The forward characteristics from Fig. 3 were analyzed using the characterization technique based on the proposed model in Sec. III. In order to determine the entire temperature and bias domains where the measured inhomogeneous devices perform like ideal diodes, the following steps were carried out:

- The bias intervals with exponential current-voltage dependence are established; based on these ranges, the ideality factor and conventional barrier at each measurement temperature are extracted.
- The widest temperature domain, for which the above established exponential forward curves have common voltage values, is identified; the resulting Arrhenius plots [Eq. (16)], for all common V_F values, are used to extract our model's parameters (p_{eff} and $\Phi_{Bn,eff}$), using an average ideality factor value.
- Using p_{eff} and $\Phi_{Bn,eff}$ in Eqs. (14) and (15), the I_F-V_F characteristics are calculated, and compared with their experimental counterparts. Thus, the entire temperature and bias range where a very good agreement between calculations and measured data is ascertained. Deviations are limited by imposing $R^2 > 95\%$.
- If experimental data are adequately matched for all considered temperatures, the process is concluded. Otherwise, the procedure is reiterated, yielding a new set of model parameters.

The discrete contact composition approach, rather than the continuous Gaussian distribution proposed by other models,[37,38] was essential in order to develop this characterization technique. It is noted that temperature ranges where the devices' electrical characteristics cannot be accurately parameterized using this technique may truly be considered "unpredictable" and should be avoided in practical applications.

Thus, sample D7 exhibited stable characteristics at all temperatures, with exponential current-voltage dependence over at least four orders of magnitude [Fig. 3(a)]. Despite this apparent uniformity, two temperature intervals with distinct effective barriers and areas were identified. In the 50 °C–150 °C domain, a $\Phi_{Bn,eff}$ of 1.58 V and p_{eff} of 2.82 were extracted. For this range, the area contributing dominantly to current conduction is approximately 17 times lower than the nominal area.

In the 200 °C–350 °C span, the effective barrier grew to 1.7 V (becoming near identical with the conventionally extracted barrier, $\Phi_{Bn,T}$), while p_{eff} decreased to 0.03. In this

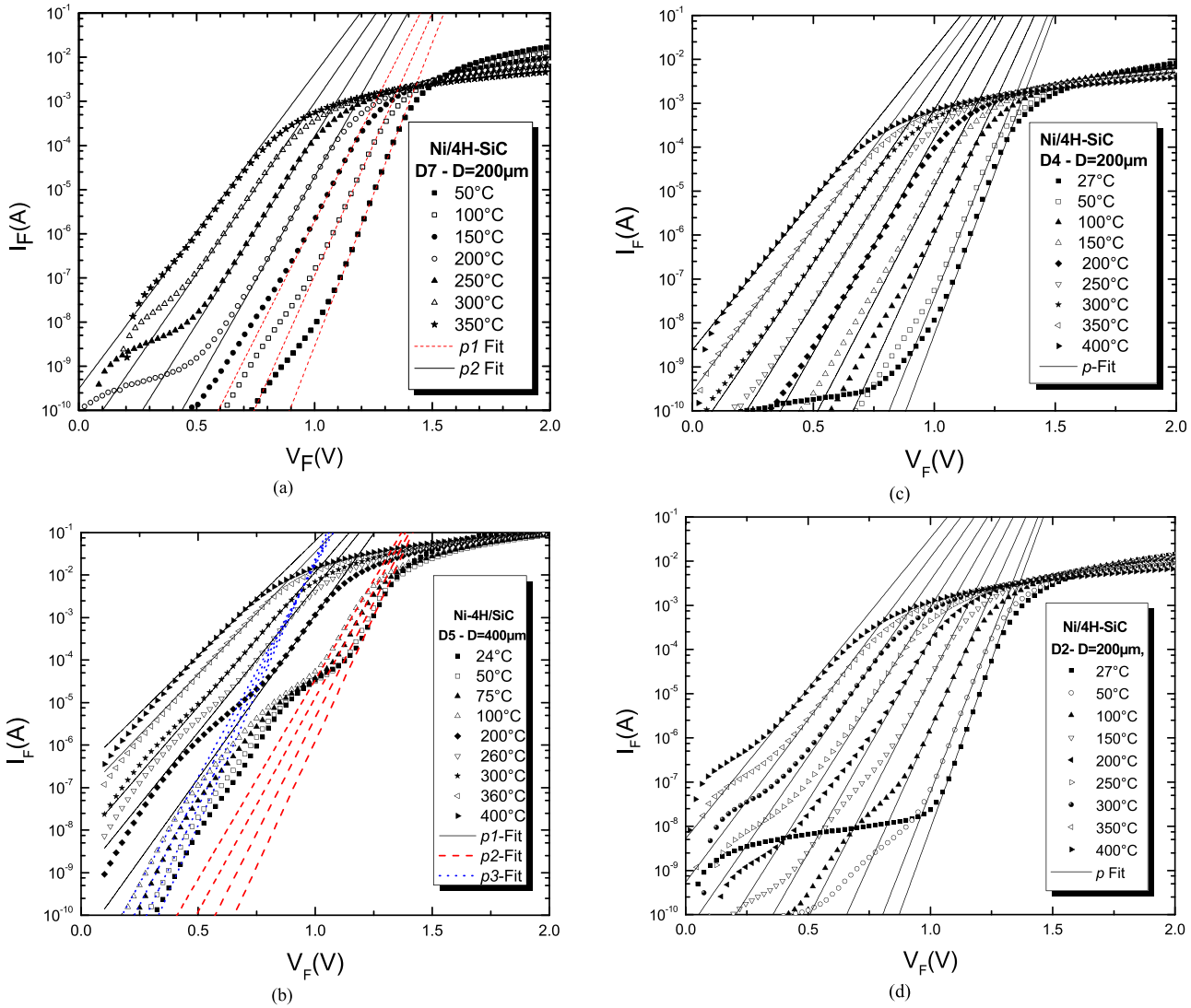

FIG. 3. Forward characteristics of Ni/SiC Schottky diodes, at different temperatures, and fitted results, using Eq. (5), for four samples.

case, it can be affirmed that the diode acts entirely homogeneously, with the whole nominal area contributing significantly to current conduction. According to the proposed model, this behavior perpetuates at all temperatures above 350 °C. Since the XRD analysis[10,55] evinced only the presence of Ni_2Si on the contact area, the real barrier height of this phase should be equal to the effective barrier extracted using our model. Furthermore, $\Phi_{Bn,T} \cong \Phi_{Bn,eff} = 1.7$ V [see model Eq. (12)]. This is very close to the desired SBH, which is $\Phi_{Bn,d} = \Phi_M - \chi = 1.73$ V, according to the Schottky-Mott theory.[10] The result was also predicted by Roccaforte *et al.*,[31] who used Tung's model to calculate Φ_{Bn}^0 for the same Ni silicide Schottky contact measured at very low temperatures. The identity between the proposed model's effective barrier, the conventional barrier, and the mean barrier in the Gaussian distribution approach, at high enough temperatures is therefore confirmed. Furthermore, these results indicate that the "pinch-off" effects evinced by the Tung model[38] do not significantly impact current flow through the diode at elevated temperatures, especially over 200 °C.

In contrast with D7, device D5 [Fig. 3(b)] exhibits visible non-uniformity on characteristics up to 260 °C. Fitting for 24 °C–100 °C was performed for both low and high bias regions in order to emphasize the versatility of the proposed characterization technique. The very low values obtained for SBH at reduced bias voltages, coupled with high p_{eff}, confirm the strong non-uniformities on the contact surface. In this case, the extremely large series resistance value for the dominant low-barrier patch shunts its current contribution at high bias voltage. At even higher voltages, parallel conduction through larger barrier regions takes precedence. While it can be stated that, even in this interval (24 °C–100 °C), D5 has bias regions with predictable quasi-ideal behavior, the narrow domains greatly restrict the device's practical uses in applications.

As measurement temperature exceeded 200 °C, the forward characteristics became more uniform, with a single region contributing to current conduction [Fig. 3(b)]. Thus, the effective barrier height increased to 1.18 V and p_{eff} decreased to 6.17. While the major current contribution was still focused in an effective area much lower than nominal (about 500 times smaller), the current-bias domain where the device behaved quasi-ideally now spanned at least 2 orders of magnitude. The analysis performed on D5 shows that

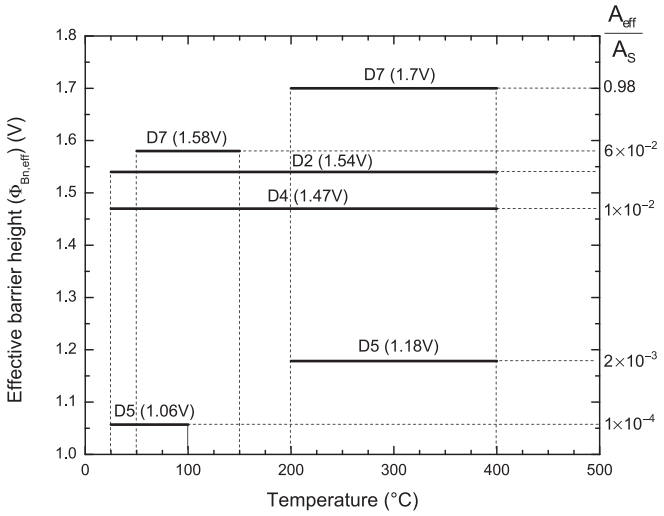

FIG. 4. Effective barrier heights and area ratios for investigated Ni/SiC samples using the *p*-parameter method ($A_{eff}/A_S = -\exp(p_{eff})$).

regions with a low barrier and area still overwhelmingly influence device current, even at 400 °C. For such devices, the extraction of conventional and mean barriers from the Gaussian distribution models[37,38] merely yields fitting parameters which normalize current flow to the nominal area, devoid of physical significance.

Sample D4 [Fig. 3(c)] does not show any visually identifiable double-barrier behavior. Fitting the forward characteristics in the entire measurement temperature range was possible using a single parameter pair ($\Phi_{Bn,eff} = 1.47$ V and $p_{eff} = 4.4$), with minor modifications to the ideality factor (between 1.12 and 1.14) in the 27 °C–150 °C domain. The same procedure was possible for device D2, this time without the need for ideality factor adjustment. A value of $p_{eff} = 2.4$ was extracted for this device.

The above mentioned results of the proposed characterization method are summarized in Fig. 4 for all samples with Ni/4H-SiC contacts. Devices D2 and D4 have a near-ideal behavior for the entire 27 °C–400 °C considered temperature range. For both D5 and D7, adequate behavior was identified in the 200 °C–400 °C domain, confirming that, as temperature increases, effective barrier heights and active areas become more stable. The considered SBH value for D5 in the 24 °C–100 °C interval (Fig. 4) was the one determined at high bias [see Fig. 3(b)].

It should be mentioned that a barrier of around 1.5 V (as is the case for D2 and D4) has been previously reported (Table I)[31,51] for annealed Ni/4H-SiC contacts measured at temperatures over 200 °C. This SBH value may suggest, that for, these samples, there are multiple stable silicide phases on the Ni/SiC Schottky contact surface.

The same analysis was performed for fabricated Pt/SiC Schottky diodes, measured in the 27 °C–250 °C interval, with results depicted in Fig. 5.

For both samples, the experimental characteristics were fitted by a single $\Phi_{Bn,eff} = 1.47$ V. D1 gave $p_{eff} = 1.37$, while for D2 $p_{eff} = 2.1$ was extracted, indicating a slight degree of contact inhomogeneity. Fitted curves in Fig. 5 are accurate above 50 °C for D1, and over the entire temperature range

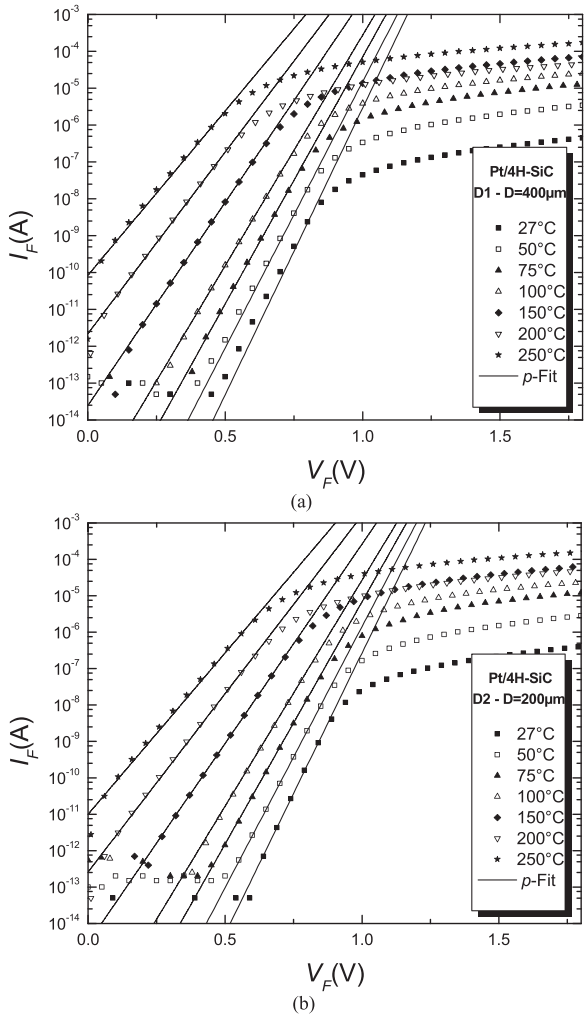

FIG. 5. Forward characteristics of Pt/SiC Schottky diodes, at various temperatures, and fitted results, for two samples with different contact areas.

for D2. In both cases, the devices exhibited stable behavior in temperature intervals spanning over 200 °C.

Table III shows the temperature and bias ranges where the investigated Schottky diodes have quasi-ideal behavior despite contact inhomogeneity.

It should be noted that the bias intervals for each device in Table III were correlated with their entire established temperature domains. If a narrower temperature range were considered, the bias interval where the device behaves near ideally would increase. For example, the D2-Ni current range can be extended over three orders of magnitude (250 nA–250 μA) by constraining the temperature interval to only 27 °C–100 °C.

TABLE III. Domains of quasi-ideal behavior for inhomogeneous experimental samples.

Device	Temperature interval	I_F Bias domain
D2-Ni	27 °C–400 °C	2 μA–100 μA
D4-Ni	27 °C–400 °C	50 nA–50 μA
D5-Ni	200 °C–400 °C	70 μA–2 mA
D7-Ni	50 °C–150 °C/200 °C–350 °C	200 nA–100 μA/50 nA–50 μA
D1-Pt	50 °C–250 °C	100 pA–25 nA
D2-Pt	27 °C–250 °C	10 pA–10 nA

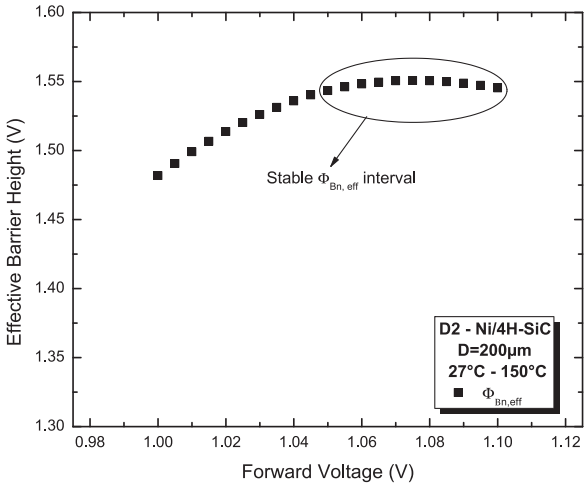

FIG. 6. Effective SBH variation with forward voltage for diode D2-Ni.

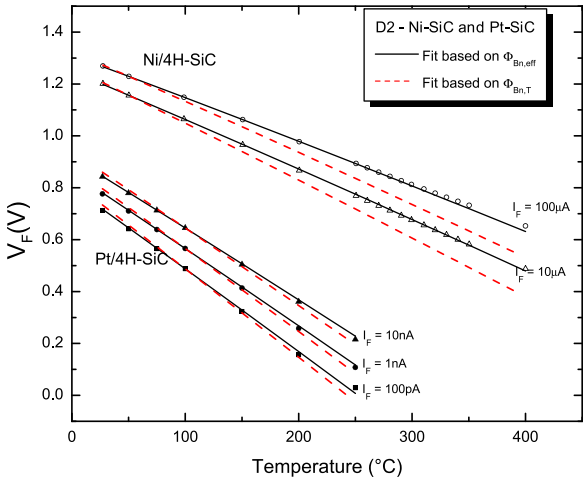

FIG. 7. Forward voltage variation with temperature for D2-Ni and D2-Pt samples at different current levels. Calculated curves are obtained using conventional and effective Schottky barrier values.

The excellent agreement between experimental and fitted data could only be achieved by a thorough consideration of accuracy criteria for obtaining effective barrier from the Arrhenius plots. While, in the literature, many results pertaining to inhomogeneous contacts stem from activation energy curves,[31,43–45,48,52] there are very few discussions regarding their relevance in the context of temperature and bias interval selection. In fact, a critical aspect is adequately choosing temperature domains and voltage levels for which the Arrhenius curves are to be plotted. For example, considering sample D2, extrapolating forward characteristics [Fig. 3(d)] at zero bias, in order to obtain the $\ln\frac{I_S}{T^2}\left(\frac{1}{T}\right)$ graph, led to unphysical results, yielding a contact area nearly ten times greater than the designed value. Hence, due to the uncontrollable nature of inhomogeneous contacts, it is preferred to use actual experimental data for Arrhenius plots, i.e., $\ln\frac{I_F}{T^2}\left(\frac{T_0}{T}\right)$ for different V_F = constant. Figure 6 depicts the extracted effective barrier variations with forward voltage for sample D2, in the 27 °C–150 °C window of analysis. A brief visual inspection of forward curves in Fig. 3(d) reveals that, for this temperature interval, an exponential I_F-V_F dependence is only achieved for common $V_F = 1.05\,V \ldots 1.1\,V$. Accordingly, the SBH obtained for this range is quasi constant (variations under 1%). For lower voltages, the $\ln\frac{I_F}{T^2}\left(\frac{T_0}{T}\right)$ curves are not linear anymore, fallaciously indicating a SBH bias dependence (Fig. 6).

The validity of our proposed model is all-the-more confirmed by the possibility to precisely fit forward characteristics over large temperature and bias ranges using parameters extracted from measurements in a much narrower region. Thus, the experimental D2 forward curves [Fig. 3(d)] were fitted up to 400 °C using parameters extracted only from measured data in the 27 °C–150 °C interval, for a bias range of 1.05 V–1.1 V (Fig. 6).

For investigated devices, the conventional barrier usually exhibited the predictable temperature variation exemplary of inhomogeneous contacts. On the other hand, $\Phi_{Bn,T}$ extraction yielded relatively temperature-stable values for D2-Ni (1.62 V ± 30 mV) and D2-Pt (1.55 V ± 15 mV). In order to establish if, in this case, the conventional SBH holds physical significance, measured and calculated $V_F(T)$ curves at several constant I_F levels were plotted in Fig. 7 for both D2 diodes. Calculations were performed using expression[1,12]

$$V_F(T) = n\Phi_{Bn} - \left[n\Phi_{Bn} + 2nV_{th0}\ln\left(\frac{T}{T_0}\right) - V_F(T_0)\right]\frac{T}{T_0}, \tag{17}$$

where Φ_{Bn} was replaced with either the abovementioned values of $\Phi_{Bn,T}$ (for dashed lines in Fig. 7) or $\Phi_{Bn,eff}$ (continuous lines—Fig. 7), determined for D2 Ni and Pt contacts.

Equation (17) was obtained from Eq. (1), written at two different temperatures (i.e., T and a reference T_0).[1,12] It is used in temperature monitoring applications to predict the temperature response of a homogeneous Schottky-diode.[1,10–13,52]

A very good agreement between measured and calculated characteristics was obtained for the effective barrier height, only. The mean square error was over five times greater when using the conventional barrier height for fitting D2-Pt plots, and in excess of 80 times for D2-Ni curves. These observations serve to further establish that the electrical behavior of an inhomogeneous diode is accurately described solely by the proposed model-extracted effective barrier and non-uniformity parameter.

V. CONCLUSIONS

This paper discussed a high-temperature application-focused technique to characterize Schottky diodes with inhomogeneous contacts. A review of multiple literature-contributions, pertaining to Schottky contact characterization, was performed, highlighting the impact of barrier non-uniformity. An inhomogeneous contact comprises patches of various barriers, which directly influence responsivity for given temperature domains. It was shown that the conventional technique, overly favored in the literature to determine the barrier height at a single temperature, cannot be reliably used for characterizing non-uniform SiC-Schottky diodes. SBH Gaussian-distribution-based approaches were

also examined, regarding model complexity and relevance at high temperature. The effect of annealing, required for obtaining high-temperature-capable SiC-Schottky diodes, on the contact surface morphology and electrical behavior was briefly presented.

Taking all these considerations into account, an effective methodology to determine temperature and bias intervals, where inhomogeneous SiC Schottky diodes operate predictably in applications, with a stable barrier height, was proposed. This process is based on a discrete parallel conduction model for non-uniform Schottky contacts. The model is suitable at elevated temperatures, where the electrical interaction, on the Schottky surface, between patches with different barriers, such as the "pinch-off" effect, is much diminished. The critical parameters obtained with the proposed characterization method are the effective SBH and non-uniformity parameter p_{eff}. Like the ideality factor, this parameter allows at-a-glance evaluation of the degree of contact inhomogeneity. Furthermore, it gives an estimate for the dominant patch area. Temperature and bias domains where an inhomogeneous contact can be modeled using constant values for these parameters represent the intervals where the Schottky diode has quasi-ideal TE electrical behavior (exponential forward characteristics) and is strongly suitable in all usual applications.

The characterization method was successfully tested on fabricated 4H-SiC Schottky diodes with annealed high-barrier Ni and Pt contacts, exhibiting varying degrees of inhomogeneity. This technique was also validated on a simulated 3-barrier structure. All I_F-V_F-T datasets of investigated Schottky structures were accurately modeled, parameterized and fitted over a large high-temperature range. Matching between the proposed model-extracted parameters and previously reported results, using existing inhomogeneity approaches, was proven. It was established that, for annealed Ni/4H-SiC contacts, there are two stable silicide phases, with barriers of around 1.5 V and 1.7 V, which influence current conduction at high temperatures. Operable domains were determined for all investigated samples. In each case, quasi-ideal behavior was identified for temperature intervals spanning 200 °C. A predictable exponential current-voltage variation over at least 2 orders of magnitude was also proven.

The physical relevance of model-extracted parameters, especially effective SBH, was further confirmed over the entire 27 °C–400 °C range by reproducing a high temperature SiC-Schottky sensor's sensitivity. Thus, using the proposed characterization technique, it was proven that silicon carbide Schottky diodes are suitable for high-temperature-specific applications, in harsh industrial environments, up to at least 400 °C.

APPENDIX: CONVENTIONAL BARRIER VARIATION LIMITS

Here, the complete steps for determining the variation limits for $\Phi_{Bn,T}$ are presented.

Taking into account that

$$\sum_{i=1}^{m}\frac{1}{a_i}=1, \tag{A1}$$

and that each exponential term in Eq. (5) is lower than 1, the conventional barrier will be greater than or equal to $\Phi_{Bn,l}$ at any temperature. At very low temperatures, where the thermal voltage, $V_{th}=\frac{kT}{q}$ (k—Boltzmann's constant, q—elementary charge), approaches zero

$$\begin{aligned}\Phi_{Bn,T}|_{V_{th}\to 0}&=\lim_{V_{th}\to 0}\left[\Phi_{Bn,l}-V_{th}\ln\sum_{i=1}^{m}\frac{1}{a_i}\exp\left(-\frac{\Delta\Phi_{Bn,i}}{V_{th}}\right)\right]\\&=\lim_{V_{th}\to 0}\left(\Phi_{Bn,l}-V_{th}\ln\frac{1}{a_1}\right)=\Phi_{Bn,l},\end{aligned} \tag{A2}$$

because

$$\lim_{V_{th}\to 0}\exp\left(-\frac{\Delta\Phi_{Bn,i}}{V_{th}}\right)=0,\quad \text{for } i=\overline{2,m}, \tag{A3}$$

and $\Delta\Phi_{Bn,1}=0$.

As a conclusion, at low temperature, the conventional barrier increases linearly

$$\Phi_{Bn,T}\cong\Phi_{Bn,l}+V_{th}\ln a_1. \tag{A4}$$

This initially linear dependence will be attenuated as temperature further increases and more terms in the sum become relevant. The upper limit for $\Phi_{Bn,T}$, considering $V_{th}\to\infty$, is

$$\Phi_{Bn,T}|_{V_{th}\to\infty}=\Phi_{Bn,l}-\lim_{V_{th}\to\infty}\left[V_{th}\ln\sum_{i=1}^{m}\frac{1}{a_i}\exp\left(-\frac{\Delta\Phi_{Bn,i}}{V_{th}}\right)\right]. \tag{A5}$$

Using l'Hôpital's rule yields

$$\begin{aligned}&\lim_{V_{th}\to\infty}\left[V_{th}\ln\sum_{i=1}^{m}\frac{1}{a_i}\exp\left(-\frac{\Delta\Phi_{Bn,i}}{V_{th}}\right)\right]\\&=\lim_{V_{th}\to\infty}\left[-\frac{\sum_{i=1}^{m}\frac{\Delta\Phi_{Bn,i}}{a_i}\exp\left(-\frac{\Delta\Phi_{Bn,i}}{V_{th}}\right)}{\sum_{i=1}^{m}\frac{1}{a_i}\exp\left(-\frac{\Delta\Phi_{Bn,i}}{V_{th}}\right)}\right].\end{aligned} \tag{A6}$$

Finally,

$$\Phi_{Bn,T}|_{V_{th}\to\infty}=\Phi_{Bn,l}+\sum_{i=1}^{m}\frac{\Delta\Phi_{Bn,i}}{a_i}=\sum_{i=1}^{m}\frac{\Phi_{Bn,i}}{a_i}\cong\Phi_{Bn,d}. \tag{A7}$$

[1]G. Brezeanu, M. Badila, F. Draghici, R. Pascu, G. Pristavu, F. Craciunoiu, and I. Rusu, in *2015 International Semiconductor Conference (CAS), Sinaia, Romania, 12–14 October* 2015, pp. 3–10.
[2]B. Ozpineci and L. M. Tolbert, IEEE Power Electron. Lett. **1**(2), 54 (2003).
[3]G. Pristavu, G. Brezeanu, M. Badila, A. Vasilica, and R. Pascu, in *2015 11th Conference on Ph.D. Research in Microelectronics and Electronics (PRIME), Glasgow, United Kingdom, 29 June–02 July* 2015, pp. 157–160.
[4]X. She, A. Q. Huang, O. Lucia, and B. Ozpineci, IEEE Trans. Ind. Electron. **PP**, 1 (2017).
[5]A. R. Hefner, R. Singh, J.-S. Lai, D. W. Berning, S. Bouche, and C. Chapuy, IEEE Trans. Power Electron. **16**, 273 (2001).
[6]R. Singh, J. A. Cooper, M. R. Melloch, T. P. Chow, and J. W. Palmour, IEEE Trans. Electron Devices **49**, 665 (2002).

[7]O. Harmon, T. Basler, and F. Björk, Bodo's Power Syst. **1**, 34 (2015).
[8]P. Gammon, in *2013 14th International Conference on Ultimate Integration on Silicon (ULIS), Coventry, UK, 19–21 March* 2013, pp. 9–13.
[9]F. Roccaforte, F. Giannazzo, F. Iucolano, J. Eriksson, M. H. Weng, and V. Raineri, Appl. Surf. Sci. **256**, 5727 (2010).
[10]G. Pristavu, G. Brezeanu, M. Badila, R. Pascu, M. Danila, and P. Godignon, Appl. Phys. Lett. **106**, 261605 (2015).
[11]G. Pristavu, G. Brezeanu, M. Badila, F. Draghici, R. Pascu, F. Craciunoiu, I. Rusu, and A. Pribeanu, Mater. Sci. Forum **897**, 606 (2017).
[12]G. Pristavu, G. Brezeanu, M. Badila, F. Draghici, R. Pascu, and F. Craciunoiu, Mater. Sci. Forum **858**, 577 (2016).
[13]R. Pascu, G. Pristavu, G. Brezeanu, F. Draghici, M. Badila, and F. Craciunoiu, Mater. Sci. Forum **821–823**, 436 (2015).
[14]G. W. Hunter, P. G. Neudeck, L. Y. Chen, D. Knight, C. C. Liu, and Q. H. Wu, Mater. Sci. Forum **264–268**, 1093 (1998).
[15]L. Baud, Ph.D. thesis, Institut National Polytechnique, Grenoble, 1995.
[16]P. M. Gammon, A. Perez-Tomas, V. A. Shah, O. Vavasour, E. Donchev, J. S. Pang, M. Myronov, C. A. Fisher, M. R. Jennings, D. R. Leadley, and P. A. Mawby, J. Appl. Phys. **114**, 223704 (2013).
[17]S. Bellone, L. Di Benedetto, and A. Rubino, J. Appl. Phys. **113**, 224503 (2013).
[18]L. Huang, F. Qin, S. Li, and D. Wang, Appl. Phys. Lett. **103**, 033520 (2013).
[19]K.-Y. Lee and Y.-H. Huang, IEEE Trans. Electron Devices **59**, 694 (2012).
[20]S. Shivaraman, L. H. Herman, F. Rana, J. Park, and M. G. Spencer, Appl. Phys. Lett. **100**, 183112 (2012).
[21]L. Boussouar, Z. Ouennoughi, N. Rouag, A. Sellai, R. Weiss, and H. Ryssel, Microelectron. Eng. **88**, 969 (2011).
[22]F. Roccaforte, F. Giannazzo, and V. Raineri, J. Phys. D: Appl. Phys. **43**, 223001 (2010).
[23]F. Giannazzo, F. Roccaforte, F. Iucolano, V. Raineri, F. Ruffino, and M. G. Grimaldi, J. Vac. Sci. Technol. B **27**, 789 (2009).
[24]I. Nikitina, K. Vassilevski, A. Horsfall, N. Wright, A. G. O'Neill, S. K. Ray, K. Zekentes, and C. M. Johnson, Semicond. Sci. Technol. **24**, 055006 (2009).
[25]A. F. Hamida, Z. Ouennoughi, A. Sellai, R. Weiss, and H. Ryssel, Semicond. Sci. Technol. **23**, 045005 (2008).
[26]M. Furno, F. Bonani, and G. Ghione, Solid-State Electron. **51**, 466 (2007).
[27]M. E. Aydin, N. Yildirim, and A. Turut, J. Appl. Phys. **102**, 043701 (2007).
[28]D. J. Ewing, L. M. Porter, Q. Wahab, X. Ma, T. S. Sudharshan, S. Tumakha, M. Gao, and L. J. Brillson, J. Appl. Phys. **101**, 114514 (2007).
[29]X. Ma, P. Sadagopan, and T. S. Sudarshan, Phys. Status Solidi A **203**, 643 (2006).
[30]L. Calcagno, A. Ruggiero, F. Roccaforte, and F. La Via, J. Appl. Phys. **98**, 023713 (2005).
[31]F. Roccaforte, F. La Via, V. Raineri, R. Pierobon, and E. Zanoni, J. Appl. Phys. **93**, 9137 (2003).
[32]B. J. Skromme, E. Luckowski, K. Moore, M. Bhatnagar, C. E. Weitzel, T. Gehoski, and D. Ganser, J. Electron. Mater. **29**, 376 (2000).
[33]D. Defives, O. Noblanc, C. Dua, C. Brylinski, M. Barthula, and F. Meyer, Mater. Sci. Eng., B **61–62**, 395 (1999).
[34]L. Zheng, R. P. Joshi, and C. Fazi, J. Appl. Phys. **85**, 3701 (1999).
[35]M. Vivona, K. Alassaad, V. Souliere, F. Giannazzo, F. Roccaforte, and G. Ferro, Mater. Sci. Forum **778–780**, 706 (2014).
[36]Y. P. Song, R. L. VanMeirhaeghe, W. H. Laflère, and F. Cardon, Solid State Electron. **29**, 633 (1986).
[37]J. H. Werner and H. Güttler, J. Appl. Phys. **69**, 1522 (1991).
[38]R. T. Tung, Mater. Sci. Eng., R **35**(1–3), 1 (2001).
[39]K. Matsuo, N. Negoro, J. Kotani, T. Hashizume, and H. Hasegawa, Appl. Surf. Sci. **244**, 273 (2005).
[40]Y. M. Abubakar, A. Lohstroh, and P. J. Sellin, IEEE Trans. Nucl. Sci. **62**(5), 2360 (2015).
[41]L. Stöber, J. P. Konrath, F. Patocka, M. Schneider, and U. Schmid, IEEE Trans. Electron Devices **63**(2), 578 (2016).
[42]S. U. Omar, T. S. Sudarshan, T. A. Rana, H. Song, and M. V. S. Chandrashekhar, IEEE Trans. Electron Devices **62**(2), 615 (2015).
[43]E. Omotoso, W. E. Meyer, F. D. Auret, A. T. Paradzah, M. Diale, S. M. M. Coelho, and P. J. Janse van Rensburg, Mater. Sci. Semicond. Process. **39**, 112 (2015).
[44]Z. Ouennoughi, S. Toumi, and R. Weiss, Phys. B: Condens. Matter **456**, 176 (2015).
[45]M. Gülnahar, Superlattices Microstruct. **76**, 394 (2014).
[46]I. Shalish, C. E. M. Oliveira, Y. Shapira, L. Burstein, and M. Eizenberg, J. Appl. Phys. **88**, 5724 (2000).
[47]A. Latreche, Z. Ouennoughi, and R. Weiss, Semicond. Sci. Technol. **31**(8), 085008 (2016).
[48]S. Toumi, A. Ferhat-Hamida, L. Boussouar, A. Sellai, Z. Ouennoughi, and H. Ryssel, Microelectron. Eng. **86**(3), 303 (2009).
[49]A. Hattab, J. L. Perrossier, F. Meyer, M. Barthula, H. J. Osten, and J. Griesche, Mater. Sci. Eng. B **89**, 284 (2002).
[50]F. La Via, F. Roccaforte, A. Makhtari, V. Raineri, P. Musumeci, and L. Calcagno, Microelectron. Eng. **60**(1–2), 269 (2002).
[51]K. V. Vassilevski, I. P. Nikitina, N. G. Wright, A. B. Horsfall, A. G. O'Neill, and C. M. Johnson, Microelectron. Eng. **83**, 150 (2006).
[52]V. Kumar, A. S. Maan, and J. Akhtar, J. Vac. Sci. Technol. B **32**, 041203 (2014).
[53]W. Kern and D. A. Puotinen, RCA Rev. **31**, 187 (1970).
[54]B. Murrel, McNair Scholars J. **10**, 83 (2006).
[55]R. Pascu, F. Craciunoiu, M. Kusko, F. Draghici, A. Dinescu, and M. Danila, in 2012 International Semiconductor Conference (CAS), *Sinaia, Romania, 15–17 October* 2012, pp. 457–460.